inter.noise
HAMBURG 2016

Truncated acoustic black hole structure with the optimized tapering shape and damping coating

Jeong-Guon IH[1]; Miseong KIM[1]; Ik-Jin LEE[1]; Jakob S. JENSEN[2]

[1] Center for Noise and Vibration Control (NoViC), Department of Mechanical Engineering, KAIST, Daejeon, Korea

[2] Technical University of Denmark (DTU), Lyngby, Denmark

ABSTRACT

The acoustic black hole (ABH) structure can be an option as a vibration damper by providing a tapered wedge at the end of a beam or plate. However, not much work has been done on design to yield an effective ABH design for such a plate. We attempt to optimize the shape of the ABH to effectively attenuate the bending vibration in the frequency bands of interest. A preliminary study is also conducted to find the relation between the vibration reduction in a whole plate and the wedge parameters, like various dimensions of the wedge and the damping material property covering the wedge, to understand the general behavior of an ABH structure. With constraints on the range of flare constant, truncated length of the ABH thin end, and thickness of damping material, the wedge profile and parameters are optimized. All computations are based on the three-dimensional finite element modeling of finite plates having ABH structure, and a surrogate model is employed to facilitate the optimization. The results show that the optimized ABH shape without damping is not much better than the non-optimized one, but that with damping exhibits a significant improvement compared to the non-optimized ones, with and without damping.

Keywords: Acoustic black hole, plate vibration, bending wave, damping layer, optimization, I-INCE Classification of Subjects Number(s): 43.2.1, 47.3

1. INTRODUCTION

The acoustic black hole (ABH) structure is a relatively new method to reduce the unwanted vibration within a main structure, which utilizes the reduction of reflected waves from the structural edge (1). If the thickness of structure decreases gradually by a power-law profile, the phase speed of bending waves propagating to the edge decreases, and the wave does not reach the edge. However, this is only true for the ideal razor sharp end, whereas, in practice, the edge truncation with a finite thickness is inevitable, which results in wave reflections. To reduce the reflection due to edge truncation, damping material covering the tapered wedge can be used (2). Many research works have been conducted for the characterization and analysis of ABH; however, not much work has been done on the design method to yield an effective ABH for the practical application. In this work, a study to optimize the finite, truncated ABH plate is done to design an effective ABH plate that will have the largest attenuation of vibration energy in the frequency bands of interest. With the practical constraints for the design parameters, the wedge shape and damping layer are optimized. The evaluation of the effectiveness of ABH is based on the magnitude of resonant peaks in the driving point mobility, and also on the mean-squared, spatially-averaged velocity. All computations in this study employ the three-dimensional finite element modeling of finite ABH plate.

[1] j.g.ih@kaist.ac.kr; miseongkim90@gmail.com; ikjin.lee@kaist.ac.kr
[2] json@elektro.dtu.dk

2. BASIC ANALYSIS BASED ON THE ACOUSTIC BLACK HOLE THEORY

2.1 General features of ABH

For a wedge comprising an edge of a plate with gradually decreasing thickness in a direction as depicted in Figure 1, the phase speed of bending waves is given by

$$c_b = \left(E\omega^2 (h(x))^2 / 12\rho(1-\nu^2) \right)^{1/4}, \tag{1}$$

where $h(x)$ is the thickness of the wedge, ω the angular frequency, E the Young's modulus, ρ the density, and ν the Poisson ratio of the plate material.

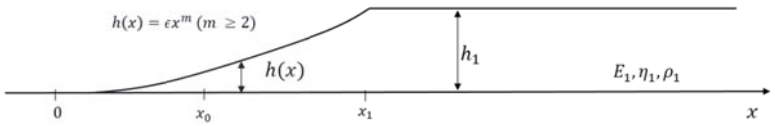

Figure 1 – The ABH plate with an infinitesimally thin edge of the tapered wedge. E_1 is the Young's modulus, η_1 the damping loss factor, ρ_1 the density of plate, and h_1 the thickness of base plate.

If the change in wavelength during the propagation within the wedge is very small, the bending wave speed approaches zero as the thickness vanishes. In this case, the wave does not reach at the end of the edge, thus preventing the wave from being reflected. A necessary condition is that the following smoothness condition is satisfied:

$$\left| \frac{d\lambda(x)}{dx} \right| = \left| \frac{1}{k^2(x)} \cdot \frac{dk(x)}{dx} \right| << 1. \tag{2}$$

Here, k is the local wavenumber, λ denotes the local wavelength, and $k_N \equiv \left| \frac{1}{k^2} \cdot \frac{dk}{dx} \right|$ is called the normalized wavenumber variation (3,4). This smoothness condition can be satisfied by the wedge with a thickness profile following the power law equation as

$$h(x) = \varepsilon x^m, \quad (m \geq 2) \tag{3}$$

where x is the distance from the wedge, $h(x)$ the local thickness of the wedge, m a positive rational number, and ε a constant.

However, in reality, an edge is truncated, as illustrated in Figure 2.

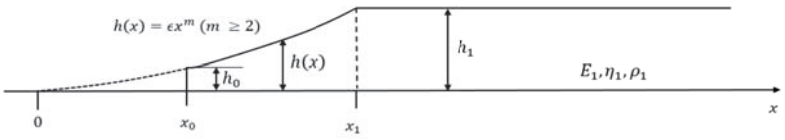

Figure 2 – The ABH plate with a truncated wedge, in which the truncation exists at x_0.

This will spoil the perfect ABH configuration, and thus results in wave reflection from the edge. The reflection coefficient can be written as

$$R(x) = \exp\left(-2 \int_{x_0}^{x} \mathrm{Im}\, k(x)\, dx \right). \tag{4}$$

Here, $k(x)$ denotes the complex wavenumber. If the truncated wedge is coated with a damping layer, the reflection coefficient decreases by increasing the imaginary part of the wavenumber. Thus, by treating the tapered wedge part with damping layer, the ABH plate becomes much more effective for the reduction of vibration energy (2). The reflection coefficient depends on the design parameters such as the wedge

shape and damping layer. Because a large amount of reflections from the edge causes an accumulation of the large vibration energy in the whole plate, the relation between the vibration reduction in the whole plate and the wedge parameters can be identified too.

2.2 Numerical model for the simulation

In the simulation, a commercial finite element code is adopted for the computation of vibration response in a finite ABH model subject to a harmonic point force P, which is normal to the surface. The quadratic isoparametric hexahedral element is used in the FE model and the mesh size is chosen to be smaller than the λ/6 of the smallest wavelength in the frequency bands of interest (5).

Figure 3 shows the geometry of a finite ABH plate for the simulation. This ABH plate with additional damping layer on tapered part is compared with two simple plates of different length as depicted in Figure 4. The geometric characteristics and material properties of ABH plate and damping material are described in Table 1. The unit point force is applied at (x_0, y_0, z_0) = (320, 107.5, 5) mm avoiding the nodal lines of the plate modes.

Table 1 – Dimensions and material properties of the plate and damping layer used in the simulation.

Geometrical parameters	Material properties	
	Plate	Damping layer
L_x=280 mm,	E_1= 190 GPa	E_2=5 GPa
L_y=195 mm,	ρ_1=7850 kgm^{-3}	ρ_2=950 kgm^{-3}
h_0=0.2 mm, h_1=5 mm	η_1=0.001	η_2=0.3
$x_1(l_t)$=50 mm	ν=0.3	

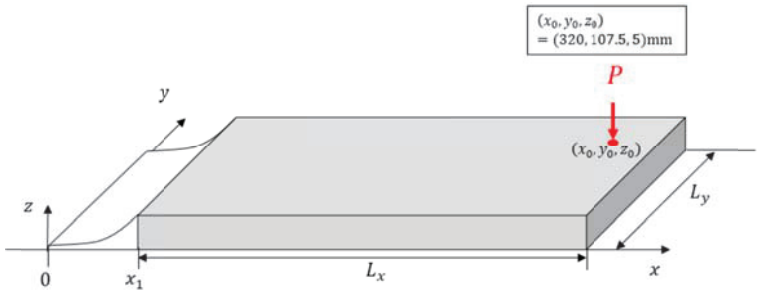

Figure 3 – Geometry of the ABH plate with the tapered part in the left side. Dimensions and properties are exhibited in Table 1. The arrow denotes the position of a normal excitation force, P.

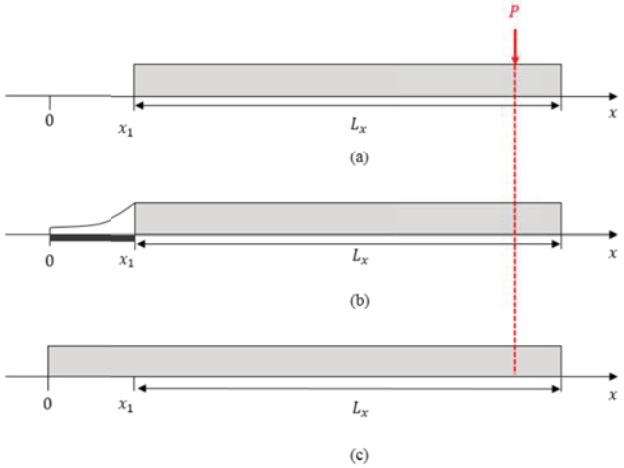

Figure 4 – Numerical test models. (a) Simple plate A, (b) ABH plate with additional damping applied at the tapered wedge, (c) simple plate C. The arrow with P denotes the normal excitation force.

2.3 Simulation results

Figure 5 shows a comparison of driving point mobility of three plate models. One can observe that the amplitudes of resonant peaks of ABH plate with additional damping layer are decreased largely above 3 kHz in comparison with the two simple plates.

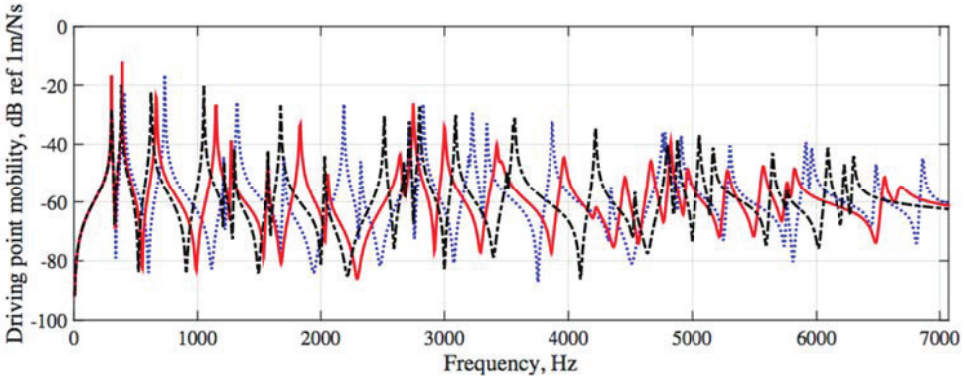

Figure 5 – A comparison of driving point mobility at three plate models as shown in Figure 4: ⋯, simple plate A; —, ABH plate with additional damping; – · –, simple plate C.

In order to compare the reduction of vibration energy in more detail, the mean-square of the spatially averaged velocity in the 1/3-octave frequency bands is calculated. As far as the frequency bandwidth is selected to be wide enough to contain at least 5 resonant peaks, this quantity reveals a steady vibration energy in the frequency band as (6)

$$\left\langle v_{\Delta}^{2}\right\rangle = \frac{1}{\Delta\omega}\int_{\omega_1}^{\omega_2}\overline{v^2}\,d\omega. \tag{5}$$

Here, $\overline{v^2}$ is the square of spatially averaged velocity, ω_1, ω_2 are the lower and upper frequency of the band, respectively, and $\Delta\omega = \omega_2 - \omega_1$. In Figure 5, one can see that the number of resonant peaks is larger than 5 above 5 kHz in the 1/3-octave band center frequency for all three plates. Therefore, two frequency bands (5 and 6.3 kHz bands) are selected as the frequency bands of interest. The mean-squared values of spatially averaged velocity in those frequency bands are numerically calculated and it can be used to analyze the vibration energy of the plate. The optimization is conducted using this value, which is called the normalized vibration energy in the frequency bands of interest.

3. OPTIMIZATION

Based on the ABH theory and the calculated normalized vibration energy, the design parameters affecting the ABH performance are selected. The base equation to express the wedge profile is the power law equation expressed as $h(x) = h_0 + \varepsilon(x - l_0)^m, (m \geq 2)$, where x is the distance from the wedge, m a positive rational number, h_0 the minimum thickness, l_0 the length of constant thickness at the end of wedge, and ε a constant. It is assumed that the maximum thickness and the length of wedge are fixed in reasonable values for practical reason. The optimization scheme is subdivided into two parts: One is the optimization of a tapered wedge profile, which defines the shape of wedge. The other is the optimization of damping layer applied to the wedge. In order to find the design variables which yield the minimum objective function, the optimization activity is conducted using a surrogate model. It is noted that the surrogate model is applicable when all outcomes of the design variables cannot be easily measured. In this work, the surrogate model employs the Kriging method using a commercial toolbox (7). The objective function is chosen as a minimum value of the mean-squared, spatially-averaged velocity, i.e., the vibrational energy of the plate, as follows:

$$\text{Min}\left(\sum_{f_c=5\text{ kHz, }6.3\text{ kHz}}\left\langle v_{f_c}{}^2\right\rangle\right). \tag{6}$$

3.1 Wedge profile

First, an ABH plate without damping layer is optimized by design variables related to the wedge profile. Figure 6 illustrates the geometric model and parameters of wedge profile in an ABH plate. The minimum thickness of the truncated part, the power law order, and the length of truncated part are selected as the design parameters that affect the ABH performance and are related to the wedge profile. Even though the smaller edge thickness gives the smaller reflection coefficient, it is practically fixed. In this work, it is fixed to be 0.2 mm.

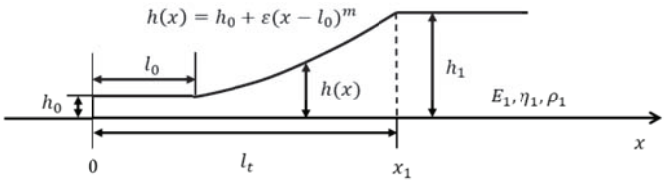

Figure 6 – Structural model and design parameters for the optimization of wedge profile of ABH plate. Here, $h(x)$ is the taper equation in the wedge, l_0 the length of truncated part, l_t the total wedge length, h_0 the minimum thickness of the truncated part, and h_1 the thickness of homogeneous plate.

The constraint of design variables is set as follows:

$$\textbf{Design variable: } m,\ l_0\,;\ \textbf{Constraints: } 2 \le m \le 6\ \&\ 0 \le l_0 < l_t.$$

The surrogate model obtained from varying the size of samples is evaluated. Figure 7 shows the surrogate model obtained from 55 samples which are selected as a valid model. As can be seen in this figure, ABH plate has minimum value of objective function in the interested frequency range when the wedge profile satisfies the normalized wavenumber variation as

$$0.45 \le \left|k_N\right| \le 0.55. \tag{7}$$

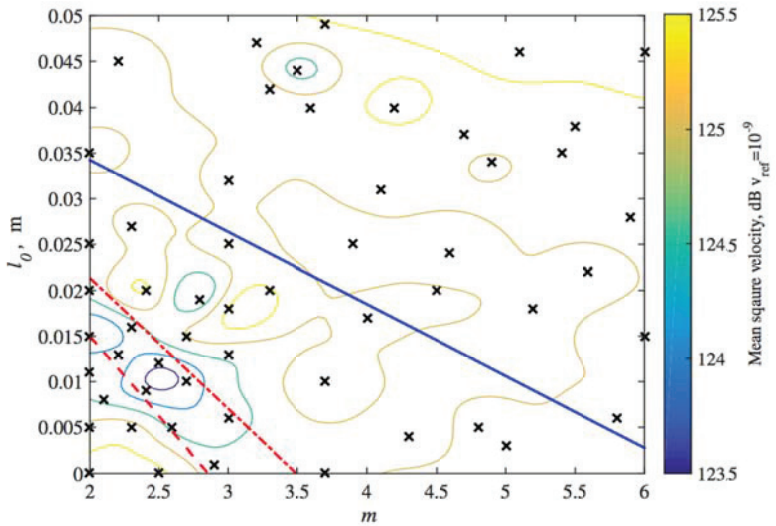

Figure 7 - Contour map of mean-squared velocity for the frequency range of interest obtained from the surrogate model made of 55 samples with normalized wavenumber variation: ×, sample points; —, $k_N = 1$; – · –, $k_N = 0.55$; – – – $k_N = 0.45$.

One can find that the wedge profile satisfying this range of normalized wavenumber variation is associated with a smaller mean-squared velocity compared to the other shape. However, it is not easy to clearly ascertain the optimal design to exist within this range because the difference from other design shapes is not significant.

3.2 Damping layer

After fixing the wedge profile following the optimum range, we have optimized the damping layer at the truncated wedge. Figure 8 shows the optimization parameters and geometry for an ABH plate with damping layer attached in the wedge part only. The thickness and length of damping layer are defined as the design variables and the thickness of damping layer is assumed constant to remove the mass loading effect. Then, the constraint of design variables is set as follows:

Design variable: h_2, l_d; **Constraint:** $\rho_2 h_2 \le 0.8\,\rho_1 h(x)$.

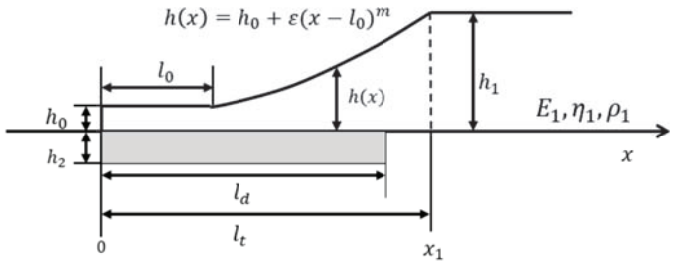

Figure 8 - Optimization model for damping layer of ABH plate, h_2 is thickness of damping layer, and l_d is length of damping layer.

Figure 9 displays the normalized vibration energy contours obtained from a validated surrogate model with the mass constraint function. As can be seen in the figure, two optimum regions can be defined by the mass of damping layer per width. One corresponds to the damping layer mass of 10-20g/m, and the other corresponds to that of heavier than 50g/m. The latter condition is achieved when the damping layer covers the whole tapered part with maximum thickness. Although the damping layers at the two optimum ranges yield similar normalized vibration energy, the damping layer with smaller mass is prefered.

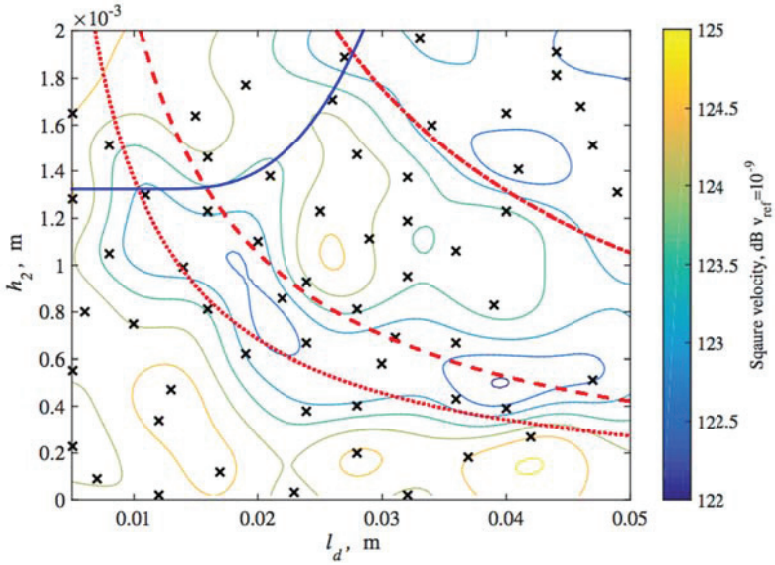

Figure 9 - Contour map of mean-squared velocity for the frequency range of interest obtained from the surrogate model made of 60 samples with normalized wavenumber variation: ×, sample points; —, $\rho_2 h_2 = 0.8\,\rho h(x)$; ⋯, $\rho_2 h_2 d_2 = 10$g/m; − − −, $\rho_2 h_2 d_2 = 20$g/m; − · −$\rho_2 h_2 d_2 = 50$g/m.

3.3 Optimization result

The ABH plate with optimized wedge profile and damping layer is compared with an initial wedge profile and two simple plates with damping layers which are optimized for each plate models. Figure 10 exhibits the various configurations used in the comparison test. Table 2 lists the calculated mean-squared, spatially-averaged velocity for each plate, and mass of damping layer per width. The table reveals that the optimized wedge profile with optimized damping layer exhibits the smallest vibration energy using the smallest amount of damping material among all plate models.

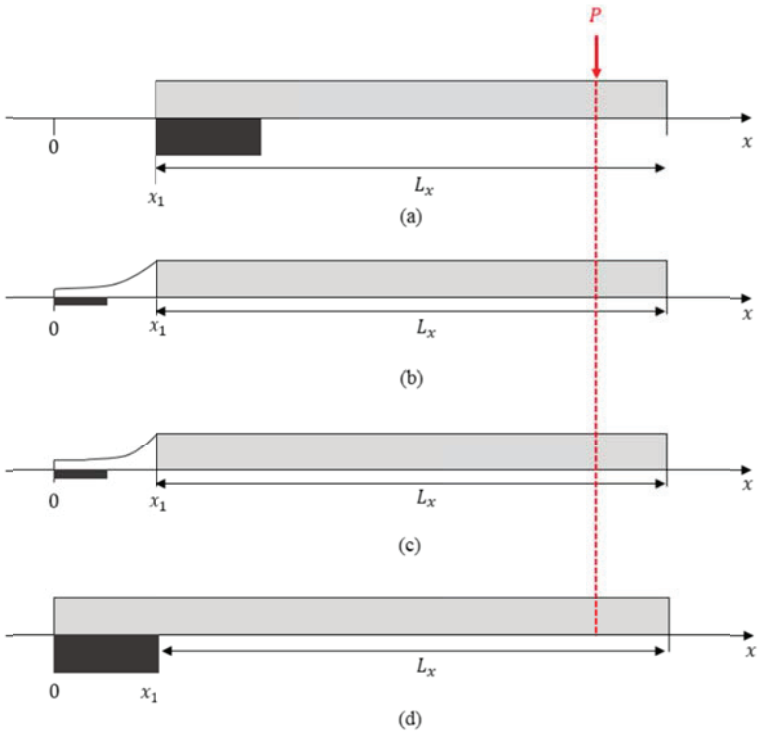

Figure 10– Comparison of plate models with damping layer coating, which is individually optimized for each plate. (a) Simple plate A, (l_d, h_2) = (50, 5) mm; (b) initial ABH plate with damping coating on the whole wedge surface, (m, l_0) = (2.0, 0 m), (l_d, h_2) = (24, 0.67) mm; (c) optimized ABH plate with a partial damping on the wedge, (m, l_0) = (2.5, 0.012 m), (l_d, h_2) = (24, 0.67) mm; (d) simple plate C, (l_d, h_2) = (50, 5) mm. *P* denotes the normal excitation force.

Table 2 – Mean-squared velocity level of each plate with individually optimized damping layer within the frequency range of interest, i.e., 4400-7070 Hz ($v_{\text{ref}} = 10^{-9}$ m/s).

Plate model		$\sum_{f_c=5\text{ kHz},\ 6.3\text{ kHz}} \langle v^2_{f_c} \rangle$	Mass density of damping layer per width ($\rho_2 h_2 d_2$)
Simple plate A	(Fig. 10(a))	124.9 dB	237.5 g/m
Initial ABH plate	(Fig. 10(b))	124.2 dB	15.3 g/m
Optimized ABH plate	(Fig. 10(c))	122.6 dB	15.3 g/m
Simple plate C	(Fig. 10(d))	124.0 dB	237.5 g/m

4. CONCLUSIONS

In this study, we design the ABH plates with a large attenuation of vibration energy in the frequency range of interest. To achieve this goal, the effect of design parameters, which would affect

the vibro-acoustic performance of the ABH structure, have been investigated numerically for the finite ABH plate. From the simulation results, it is observed that the thickness profile of the tapered part and the damping layer affect the acoustic black hole effect significantly, and, thus, it provides the necessity for the optimization. Then, the thickness profile of the tapered wedge and the damping layer applied on the wedge surface are attempted to be optimized. It is seen that the fully optimized ABH plate from this study yields about 2-dB smaller normalized vibration energy than the initial non-optimized ABH plate as well as the simple plates without ABH structures, at least within the frequency range of interest.

ACKNOWLEDGEMENTS

This work was partially supported by the BK21 Plus Project and the NRF grant (No. 2010-0028680).

REFERENCES

1. Mironov, MA. Propagation of a flexural wave in a plate whose thickness decreases smoothnly to zero in a finite interval. Sov Phy Acoust. 1988;34:318-319.
2. Krylov, VV, Tilman, FJBS. Acoustic black holes for flexural waves as effective vibration dampers. J Sound Vib. 2004;274:605-619.
3. Kinsler, LE, Frey, AR, Coppens, AB, Sanders, JV. Fundamentals of Acoustics. 4th ed. John Wiley & Sons, New York; 2000.
4. Feurtado, PA, Conlon, SC, Semperlotti, F. A normalized wave number variation parameter for acoustic black hole design. J Acoust Soc Am. 2014;136:148-152.
5. Marburg, M. Six boundary elements per wavelength: is that enough? J Comp Acoust. 2002; 10:25-52.
6. Cremer, L, Heckl, M, Petersson, BAT. Structure-borne Sound; Structural Vibrations and Sound Radiation at Audio Frequencies. 3rd ed. Springer-Verlag, Berlin; 2005.
7. Nielsen, HB, Lophavern, SN, Søndergaard, J. DACE: a Matlab Kriging Toolbox. Tech. Univ. Denmark, Lyngby, Denmark; 2002.